34th Annual International Conference of the IEEE EMBS
San Diego, California USA, 28 August - 1 September, 2012

Determination of Vessel Wall Dynamics by Optical Microsensors

Dominic Ruh[1], Stanislav Sherman[1], Michael Theodor[1], Johannes Ruhhammer[1], Katharina Foerster[2]
Claudia Heilmann[2], Friedhelm Beyersdorf[2], Hans Zappe[1], *Member, IEEE*, and Andreas Seifert[1]

***Abstract*— Spectralphotometric measurement methods as, for example, pulse oximetry are established approaches for extracorporeal determination of blood constituents. We measure the dynamics of the arterial distension intracorporeally thus extending the scope of the method substantially. A miniaturized opto-electronic sensor is attached directly to larger arteries without harming the vessel. The transmitted light through the arteries shows a linear correlation with the pulsatile expansion in theory as well as in experiments. Intra-arterial blood pressure also shows a linear interrelationship with the optical signal. Measurements of blood vessel wall dynamics has great potential to quantify arteriosclerosis by this new and innovative approach.**

I. Introduction

Cardiovascular diseases (CVDs) comprise various types of disorders that cause the highest mortality rate worldwide [1]. Most CVDs are related to the vascular system, known as *arteriosclerosis*. In the course of arteriosclerosis the walls of large and medium-sized elastic and muscular arteries alter pathologically leading to a stiffening of the arterial wall and hence to a decreasing arterial distension [2].

So far, the mechanical properties of blood vessels have been investigated only in *in vitro* or in acute *in vivo* studies [3], [4]. In contrast, our research focuses on *miniaturized implantable* sensor systems that measure the dynamics of the arterial expansion thus the distensibility of the artery *extravascularly*. The technique provides diagnostic data to support the therapy of arteriosclerosis *continuously* over *long periods of time* [5].

The measurement principle and a sketch of the sensor are outlined in Section II. The theory underlying the measurement principle is derived in Section III. Section IV introduces the sensor design while the fabrication technology is briefly summarized in Section V. The in vivo data of our sensor system are compared to data of an intra-arterial blood pressure sensor as well as simultaneously recorded electrocardiograms (ECG) in Section VI. The measured data of Section VI is discussed in Section VII according to the theory of Section III.

II. Approach

The developed implantable Micro-Opto-Electro-Mechanical System (MOEMS) measures the dynamics of the blood vessel's expansion. The measurement principle is based on a change in transmission caused by an extended optical path during the blood vessel distension, a so-called photoplethysmogram (PPG).

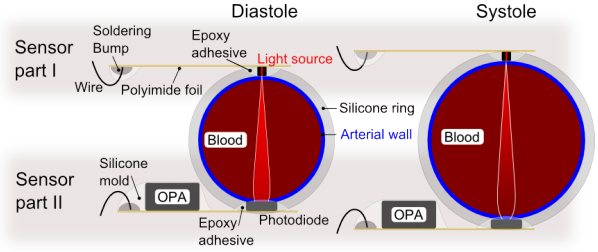

Fig. 1. System design: Two highly elastic silicone stripes diametrically oppose the two sensor parts at the artery. The sensor parts are equipped with optoelectronics to measure intensity variations in transmission caused by the distending artery.

The sensor consists of two parts that are diametrically opposed at the artery and fixed with two silicone stripes, as shown in Figure 1. Each sensor part is composed of a flexible polyimide substrate that is equipped with Light-Emitting-Diodes (LEDs) as light sources, and photodiodes (PDs) with corresponding operational amplifiers (OPAs) as sensors to measure the intensity variations induced by expansion.

III. Theory

In this Section, we show that the signal of the developed sensor is linearly related to the arterial expansion. Figure 2 introduces the definitions necessary to describe the measurement principle. With every cardiac cycle, a pressure wave starts propagating through the vascular system. As a response the arterial wall expands, leading to a longer optical path and hence to a temporally varying intensity. Neglecting scattering

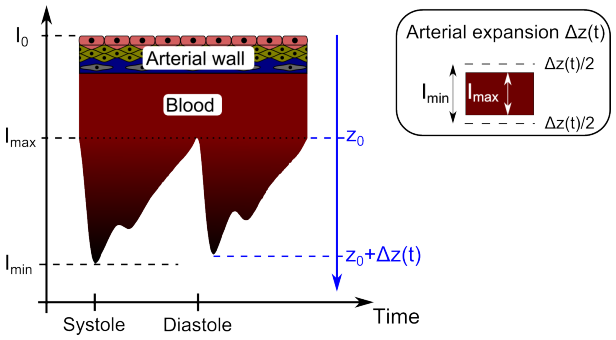

Fig. 2. Measurement principle: Intensity variations due to volumetric changes of the artery during two cardiac cycles.

[1]Department of Microsystems Engineering (IMTEK), University of Freiburg, Georges-Koehler-Allee 102, 79110 Freiburg, Germany, Email: dominic.ruh@imtek.uni-freiburg.de
[2]Cardiovascular Surgery, University Medical Center, Freiburg, Germany

effects, the change in intensity is described by Beer's law. The maximum detectable intensity I_{max} is described by

$$I_{max} = I_0 \cdot \exp(-\alpha z_0), \tag{1}$$

where I_0 denotes the input intensity, α the absorption coefficient and z_0 the blood vessel diameter at diastole. The temporally changing optical path length $\Delta z(t)$ leads to a time varying intensity $I(t)$ of

$$I(t) = I_0 \cdot \exp(-\alpha(z_0 + \Delta z(t))). \tag{2}$$

Dividing Equation (1) by Equation (2) leads to

$$\frac{I_{max}}{I(t)} = \frac{I_0 \cdot \exp(-\alpha z_0)}{I_0 \cdot \exp(-\alpha(z_0 + \Delta z(t)))} = \exp(\alpha \Delta z(t)). \tag{3}$$

An increasing optical path length leads to a reduced $I(t)$, while the ratio $I_{max}/I(t)$ increases. Small diameter variations lead to small variations of $I_{max}/I(t) \geq 1$. A first order power series expansion of $\ln(I_{max}/I(t))$ around $I_{max}/I(t) = 1$ yields,

$$\ln\left(\frac{I_{max}}{I(t)}\right) = \frac{I_{max}}{I(t)} - 1 + R_2\left(\frac{I_{max}}{I(t)}\right), \tag{4}$$

where R_2 is the second order Lagrange form of the residual. Several *in vivo* experiments conducted in this work have shown that the measured intensity variations due to physiological blood vessel expansions are less then 10 %, such that $R_2(1.1) = 5‰$. The linear relationship between the measurement signal and the arterial expansion is given by

$$\Delta z(t) \approx \frac{1}{\alpha}\left(\frac{I_{max}}{I(t)} - 1\right). \tag{5}$$

The sensitivity of the device is inversely related to the absorption coefficient α.

IV. System Design

Since the sensor system measures the arterial expansion the design goal is to avoid stiffening the artery by the mechanical stiffness of the sensor itself. As the Young's modulus of the silicone stripes ($E_{stripes} = 0.06$ MPa) is much smaller than that of the blood vessel ($E_{artery} = 0.6 - 2$ MPa) the sensor does not limit the blood vessel in its expansion, which is up to 500 µm for an artery of 5 mm in diameter. The molded zipper-like structures in the silicone stripes interlock with openings in the two sensor parts (20 x 1.3 x 14 mm^3 (width x height x depth)) thereby opposing the sensor parts diametrically at the artery, as shown in Figure 3. The signal-to-noise ratio of the optical signal is mainly affected by the sensor's optoelectronics. The intensity of two LEDs with emitting wavelengths of $\lambda_1 = 650$ nm and $\lambda_2 = 910$ nm and an edge length of 310 µm (JENOPTIK AG) is recorded by two photodetectors with an edge length of 900 µm. A good signal-to-noise ratio is achieved by using III-V semiconductor photodiodes (JENOPTIK AG) with sensitivities of 0.42 A/W at 660 ± 45 nm and 0.61 A/W at 880 ± 58 nm. The narrow band sensitive photodiodes enable operation at two wavelengths simultaneously and thus to measure oxygen saturation by absorption spectroscopy in a later stage of the project.

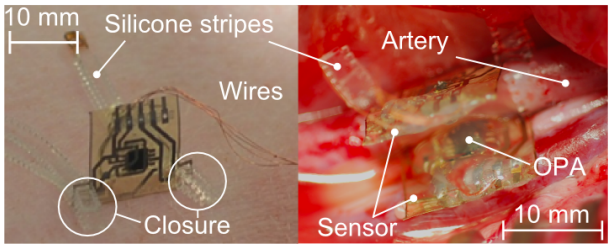

Fig. 3. Left: One sensor part before implantation. Right: Diametrically aligned sensor parts wrapped around the artery of a five months old domestic pig during surgery.

The photocurrents are amplified on chip by transimpedance amplifiers (OPA-380, Texas Instruments) and connected to a data acquisition card (National Instruments USB-6251) by wires. All electronic components are sealed by silicone (MED-1000, Nusil).

V. Fabrication

The lightweight, flexible and biocompatible polyimide substrate is manufactured by standard MEMS fabrication techniques. Photolithographically structured Pt-Au-Pt conductor paths are embedded between two 8 µm thin polyimide foils, which provide an encapsulation and act as the substrate.

Pick-and-place equipment mounts the optoelectronics on opened connector pads of the polyimide substrate with high precision. The backside of the chips is connected by conductive adhesive (EPO-TEK® H20s) while the front side is ball-wedge bonded to the substrate. A biocompatible, optical epoxy adhesive (EPO-TEK® 302-3M) serves as a robust package for the fragile optoelectronics. This packaging technique allows operation of the sensor system for several hours during surgery.

VI. Measurements & Results

Together with an intra-arterial pressure sensor as reference, the sensor is applied at the carotid artery of a five month old domestic pig under surgery. As a second reference we recorded the ECG. All data was sampled at a frequency of $F_S = 100$ kHz. Figure 4 shows the recorded signals and the reference blood pressure, as measured by an intra-arterial tip-catheter (Johnson & Johnson Codman-ICP).

Since every cardiac cycle reflects a shock wave propagation [6], we illustrate all measured data in the Fourier domain, thereby simplifying to separate the signal from the noise. The power spectral density (PSD) for each sensor is calculated by

$$S_X(f) = \frac{1}{2\pi}\frac{\left|\sum_{n=1}^{N} x_n w_n e^{-j2\pi f/F_S n}\right|^2}{\|w\|^2}. \tag{6}$$

The sum in the numerator describes the discrete Fourier transform of the dataset x_n. A Hann-Window w_n with size of the dataset N tapers the data. The sampling frequency is given by F_S, while the frequency is denoted by f. Before we analyse the two optical sensor signals in detail, we complete the picture by comparing the reference sensors with the measured data of our optical sensor.

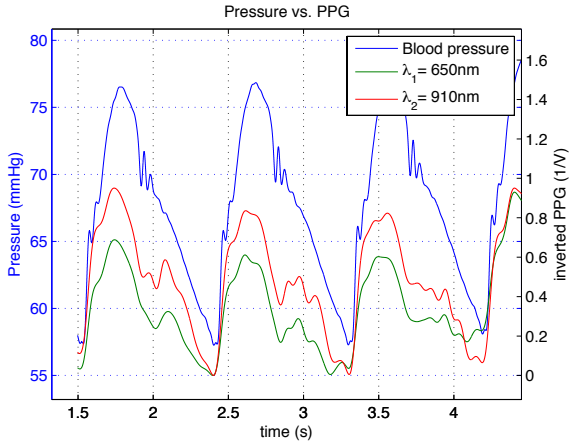

Fig. 4. Overview of the sensor signals. Three pulses recorded by an intra-arterial tip-catheter (blue) and the two normalized inverted optical signals at 910 nm (green) and 650 nm (red)

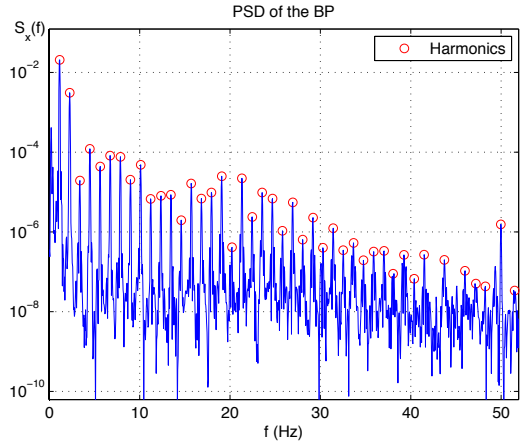

Fig. 6. Power spectral density of the intra-arterial tip-catheter.

The overtones which occur at multiples of the heart-rate, ∼1.1 Hz, dominate all four power spectral densities. In the ECG signal (Figure 5), overtones occur up to a frequency of 40 Hz. Higher frequencies are damped by the bandpass of the ECG amplifier. The PSD of the intra-arterial tip-catheter shows a similar bandwidth but lower amplitudes at higher harmonics, which can be seen in Figure 6. In comparison to the PSD of the intra-arterial tip-catheter, the power of the PPGs is concentrated in lower frequency overtones. The bandwidth of the PPGs shows up in the range of 12 Hz. The power-spectral-density of each stage of the cardiovascular system is a low-pass filtered version of the previous stage.

The power in both PPG signals is almost identically distributed in the overtones up to 12 Hz, though the sensor operating at 910 nm (Figure 7) shows values that are two orders of magnitude higher than the sensor working at 650 nm (Figure 8). In particular, the overtone at ∼3.5 Hz can not be resolved by the sensor operating at 650 nm. Furthermore, the sensor working at 650 nm shows a peak at a frequency of ∼50 Hz. In sum, the signal-to-noise ratio of the sensor working at 910 nm is better than the signal-to-noise ratio of the sensor operating at 650 nm.

The arterial distension is in the range of several hundred microns which makes it difficult to measure during surgery. Therefore we proof the linearity of the developed sensor system indirectly by plotting the measured intra-arterial pressure versus the optical sensor signal.

In a first order approximation, the arterial wall obeys Hook's law $\Delta p = E_p \cdot \varepsilon$, thus relating the circumferential strain $\varepsilon = \alpha \cdot \Delta z(t)$ linearly to the intra-arterial pressure Δp, where E_p is the pressure-strain modulus [4]. As long as the derived theory of Section III is valid, the pressure-strain plot shows a linear correlation as well.

According to its bandwidth, the 910 nm sensor signal is low-pass filtered at 12 Hz and cut into single pulses. These single pulses are processed according to Section III and plotted against the 40 Hz low-pass filtered pressure signal. Figure 9 exemplifies the linear correlation of the two signals and the calculated linear least-squares fit of one cardiac cycle. We calculated the slope of the fit over 21 cardic cycles, yielding 474 ± 60 mmHg.

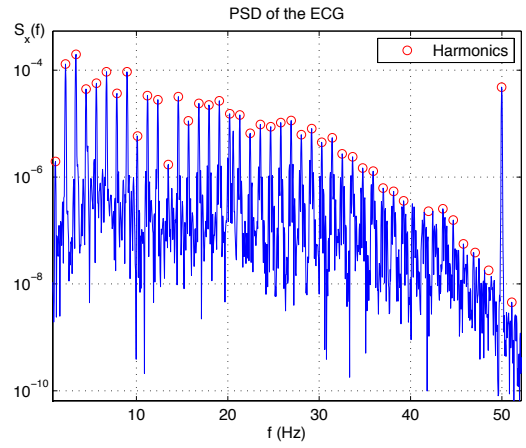

Fig. 5. Power spectral density of the ECG.

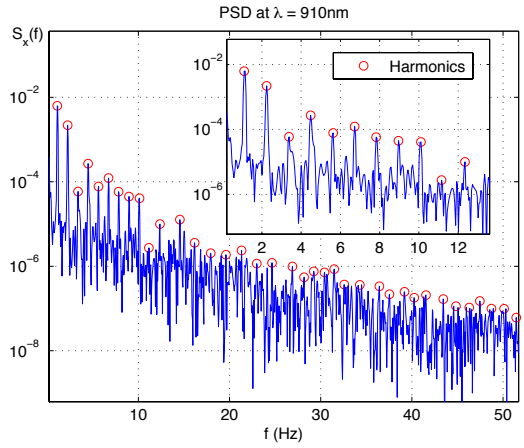

Fig. 7. Power spectral density of the PPG measured at 910 nm wavelength.

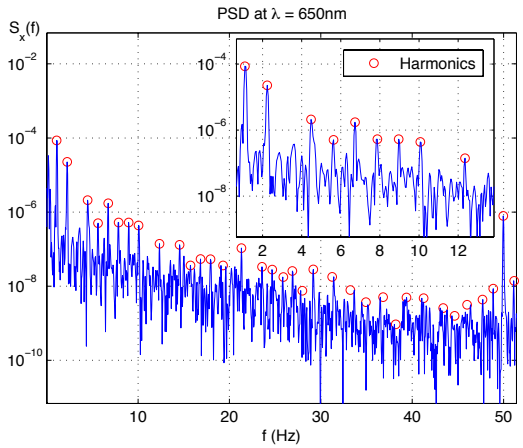

Fig. 8. Power spectral density of the PPG recorded at 650 nm wavelength.

VII. Discussion

Aside from the dissipative nature of the cardiovascular system, the detailed analysis of the sensor signals in the frequency domain in Section VI reveals that the signal-to-noise ratio of the optical sensor working at 910 nm is superior to the sensor operating at 650 nm. This is explained by the following three facts:

- The absorption coefficient of blood is wavelength dependent $\alpha(\lambda_2 = 910)/\alpha(\lambda_1 = 650) \approx 3.3$ [7]. According to Equation 5 the sensor working at 910 nm is more than three times as sensitive as the sensor operating at 650 nm.
- The sensitivity of the 910 nm PD is 0.61 A/W whereas the 650 nm PD has a sensitivity of only 0.42 A/W.
- The sensor operating at 650 nm is disturbed by ambient light (380 – 750 nm) which can be seen from the 50 Hz peak in Figure 8.

The theory derived in Section III neglects three effects that may modulate the intensity beyond that due to the change in optical path length. If scattering cannot be neglected, Beer's law has to be replaced by the radiation transfer equation [8]. The thinning of the arterial wall due to its expansion is not taken into account, nor are temporal variations of the absorption coefficient. The investigation of these second order effects will lead to a better understanding of the sensitivity of the measurement system and therewith to an absolute calibration of the developed MOEMS.

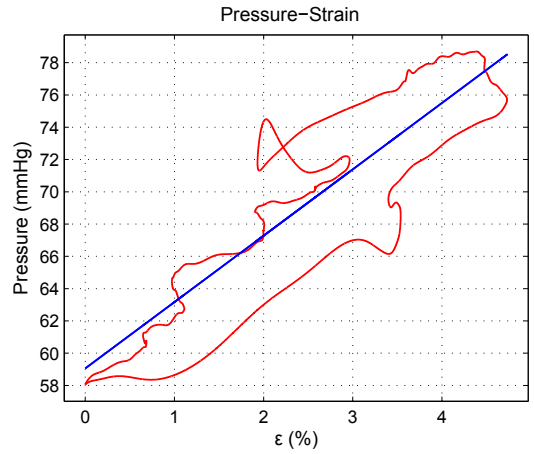

Fig. 9. Pressure-Strain curve (red) and the linear fit (blue) of one cardiac cycle.

Most probably, the hysteresis in Figure 9 is due to the viscoelasticity of the arterial wall and not a measurement error of the developed sensor system. The precision of the linear correlation between intra-arterial pressure and optical sensor signal was shown by processing 21 single pulses, yielding an error of ∼12 %.

VIII. Outlook

In this paper we presented an implantable MOEMS capable of measuring the dynamics of the arterial extension qualitatively.

Acknowledgment

We thank the JENOPTIK AG for their support concerning optoelectronics as well as Dipl.-Ing. Tim Boretius, Dipl.-Ing. Juan Ordonez and Dr.-Ing. Martin Schuettler of the Laboratory for Biomedical Microtechnology at IMTEK.

References

[1] World Health Organization, "Cardiovascular disease Fact sheet N317." [Online]. Available: http://www.who.int/mediacentre/factsheets/fs317/en/index.html (last checked: 2012/06/03).

[2] F. Epstein and R. Ross, "Atherosclerosis - an inflammatory disease," *New England Journal of Medicine*, vol. 340, no. 2, pp. 115–126, 1999.

[3] L. H. Peterson, R. E. Jensen, and J. Parnell, "Mechanical properties of arteries in vivo," *Circulation Research*, vol. 8, no. 3, pp. 622–639, 1960.

[4] T. Imura, K. Yamamoto, T. Satoh, K. Kanamori, T. Mikami, and H. Yasuda, "In vivo viscoelastic behavior in the human aorta," *Circulation Research*, vol. 66, no. 5, pp. 1413–1419, 1990.

[5] J. Fiala, P. Bingger, K. Foerster, C. Heilmann, F. Beyersdorf, H. Zappe, and A. Seifert, "Implantable Sensor for Blood Pressure Determination via Pulse Transit Time," in *Sensors, 2010 IEEE 9th Annual IEEE Conference on*, 2010, pp. 1226–1229.

[6] P. R. Painter, P. Edén, and H.-U. Bengtsson, "Pulsatile blood flow, shear force, energy dissipation and Murray's Law." *Theoretical biology & medical modelling*, vol. 3, p. 31, Jan. 2006.

[7] Scott Prahl, "Optical Absorption of Hemoglobin," 1999. [Online]. Available: http://omlc.ogi.edu/spectra/hemoglobin/index.html (last checked: 2012/06/03).

[8] T. Vo-Dinh and B. R. Masters, "Biomedical Photonics Handbook," *Journal of Biomedical Optics*, vol. 9, no. 5, p. 1110, 2004.

[9] J. Dupire, M. Abkarian, and A. Viallat, "Chaotic Dynamics of Red Blood Cells in a Sinusoidal Flow," *Physical Review Letters*, vol. 104, no. 16, pp. 1–4, Apr. 2010.